Dominance of the spin-wave contribution to the magnetic phase transition in FeRh

R. Y. Gu and V. P. Antropov
Condensed Matter Physics, Ames Laboratory, Ames, Iowa 50011, USA
(Received 28 January 2005; revised manuscript received 18 April 2005; published 5 July 2005)

Density functional calculations are performed to investigate the phase transition in FeRh alloy. The effective exchange coupling, the critical temperature of magnetic phase transition, and the adiabatic spin wave spectrum have been obtained. Different contributions to the free energy of different phases are estimated. It has been found that the antiferro-ferromagnetic transition in FeRh occurs mostly due to the spin wave excitations.

DOI: 10.1103/PhysRevB.72.012403 PACS number(s): 75.30.Kz, 71.15.Mb, 75.50.Bb

The antiferromagnetic (AFM)-ferromagnetic (FM) phase transition in FeRh with the ordered CsCl structure has been intensively studied both experimentally and theoretically. This transition occurs at $T_{tr} \approx 340$ K without any accompanying structural changes,[1] although there is an abrupt 1% volume expansion. At low temperatures the magnetic configuration of FeRh is the type II AFM phase [successive layers of (111) Fe planes AFM coupled] with moments $3.3\mu_B$ on Fe atoms (Rh atoms are nonmagnetic). Above T_{tr} in the FM phase magnetic moments are $3.2\mu_B$ on Fe atoms, $1.0\mu_B$ on Rh atoms, and the Curie temperature is $T_C \approx 670$ K.[2] In addition, it was found that T_{tr} is increased with pressure.[3,4] The AFM-FM transition can also be induced by applying external magnetic field, whose critical value at zero temperature is about 300 kOe and becomes smaller at higher temperatures,[5] making this material a natural magnetic multilayer with a large magnetoresistance effect.

Early theories of this transition based on the exchange-inversion model,[6] which assumes a change of sign for the exchange parameter at some volume, cannot account for the experimental observation of the large entropy changes at T_{tr}.[5,7–9] After discovering that the electronic specific heat in the FM phase is nearly four times larger than in the AFM phase, Tu *et al.*[10] proposed that the change of the band electron entropy plays a major role in this transition. However, they used iron-rich alloys where the value of the specific heat is very sensitive to the concentration.[11] Consecutive dielectric function measurements[12] demonstrated that the band structure of FeRh is not drastically modified during the AFM-FM phase transition.

First-principles band-structure calculations were also carried out to study this transition. Earlier calculations[13] did not compare the relative stability of the AFM and FM states. Moruzzi and Marcus[14] confirmed that the type II AFM structure is the ground state, while the FM structure represents another stable solution with the total energy nearly $\Delta E = 2$ mRy/atom higher at a larger volume. Similar results were obtained in Refs. 15 and 16. However, the energy difference ΔE obtained in these calculations appears to be much larger than the experimental data and, overall, these studies did not provide any convincing explanation of the nature of this transition. The experimental ΔE, deduced either from the latent heat $T_{tr}\Delta S$ or from the critical magnetic field at zero temperature,[5] is about 0.2 mRy/atom, which is an order of magnitude smaller than the calculated value. On the other hand, while in Ref. 14 the calculated equilibrium lattice constant in the FM state is only 0.5% larger than in the AFM state, the energy of the latter remains lower than the energy of the FM state until the lattice constant is increased by 3%. The authors[14] proposed that the zero-point lattice vibrations can correct the total energy result. However, from the Debye temperature Θ_D calculated in that paper, one can find that the correction due to zero-temperature vibration energy $E_0 = 9k_B\Theta_D/8$ is nearly two orders of magnitude smaller than the calculated ΔE. Gruner *et al.*[16] investigated the thermodynamic behavior of the system within the Ising model and found that at T_{tr} the free energy, gained due to thermoexcitation in the FM state, is nearly 0.02 mRy/atom larger than that in the AFM state. So, they proposed that it is this thermoexcitation that drives the transition. However, the magnitude of their free energy change appears too small to compensate the internal energy loss for the transition to occur. So far, in spite of many years of research, there has been no convincing explanation of the nature of the phase transition in FeRh.

In this paper we study this transition using first principles calculations and the non-collinear version of the linear muffin-tin orbital method in the atomic-sphere approximation (LMTO-ASA). In the local spin density approximation (LSDA) we use the von Barth–Hedin potential, and for the nonlocal corrections the Langreth-Mehl-Hu functional,[20] the relativistic effects, and the combined corrections[19] are included. For the radii of atoms, the ratio $R_{Rh}/R_{Fe} = 1.03$ is used. The self-consistent calculations are performed for the different lattice parameters for FM and AFM states using a spin spiral approach. The gradient corrections are expected to be important in Fe-rich BCC-based systems due to the well-known fact that LSDA-ASA predicts, for instance, the wrong ground state of pure Fe.[17,18] Using electronic density of states (DOS) and exchange parameters, we calculate the free energy change of the AFM and FM states. Various thermal quantities related to the AFM-FM transition, including the transition temperature, its pressure dependence, the entropy, and the specific heat changes, are calculated and compared with the corresponding experiments. According to our calculations, the AFM-FM transition in FeRh appears primarily due to the magnon (spin wave) excitations.

Figure 1(a) shows the calculated energy of the AFM and FM states. In LSDA the equilibrium Wigner-Seitz radius R_{WS} for the AFM (FM) phase is 2.767 (2.780) a.u., which is smaller than the previous nonrelativistic result 2.782

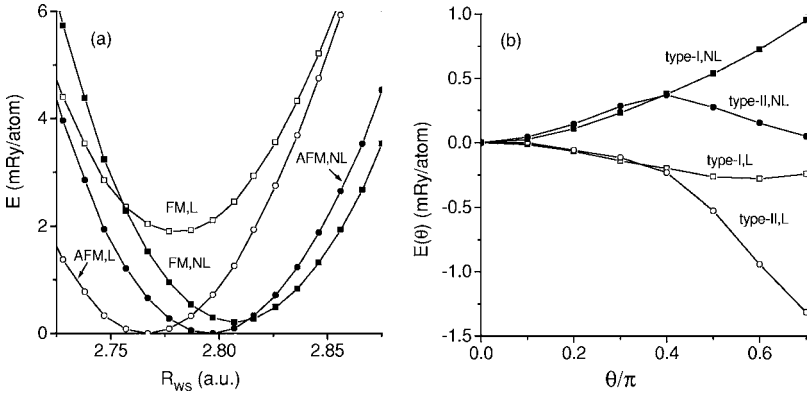

FIG. 1. The total energy obtained in the local (L) and nonlocal (NL) approximations, represented by open and solid symbols. The total energy for (a) AFM (circles) and FM (squares) states as a function of R_{WS} and (b) the type I (squares) and type II (circles) non-collinear states as a function of the spin spiral angle θ. R_{WS} is fixed at the equilibrium value of the FM state.

(2.798) a.u. (Ref. 14) [our nonrelativistic result is 2.789 (2.803) a.u.]. The energy difference between the AFM and FM states at their respective equilibrium R_{WS} is 1.89 mRy/atom. With nonlocal corrections this energy difference is reduced to 0.206 mRy/atom, which is in much better agreement with the experimental value 0.196 mRy/atom.[5] Other results are listed in Table I.

Only collinear AFM and FM configurations were observed in the experiments. In our calculation, however, we found that without nonlocal corrections the FM configuration is not a locally stable state with respect to the magnetic moment deviations, as is shown in Fig. 1(b) (two kinds of noncollinear configurations are considered). In both noncollinear configurations the Fe atoms are divided into two sublattices, identical to that in the type I [successive (001) Fe layers belong to the different sublattices] and type II AFM states with the angle θ between Fe magnetic moments from the different sublattices, while the moments of Rh atoms are parallel to the sum of the Fe moments. Such instability of the FM state is removed if the nonlocal corrections are taken into account. Results from Fig. 1 suggest that the nonlocal corrections are important in FeRh and should be taken into account in the total energy calculations.

To describe the low-energy magnetic excitations we used the traditional Heisenberg model approach which represents the most celebrated adiabatic approach in the magnetism theory. To obtain parameters of this model one has to make two important approximations. The first one is the assumption that the spin rotational degrees of freedom are slow when compared to the typical electronic frequencies.[21,22] On this stage, the time variation of the charge density is neglected. In FeRh it can be justified by comparing the electronic d-band width ($W \sim 0.5$ Ry) with the exchange energy ($J \sim 1$ mRy) (see Table II). A second important approximation is the assumption of "fixed amplitude" of the atomic magnetic moment. This is the dynamic rigid spin approach which is the *sine qua non* for any RPA type of treatment. This step assumes that one can neglect Stoner excitations in the description of the finite temperature magnetism. The smallness parameter in this case is the ratio between on-site Stoner and intersite exchange parameters J_{ij}/I. This is also a smallness criteria of the long-wavelength approximation[23] which is used in our calculations of the effective exchange parameters.[24] Due to this coincidence, our theory is consistent in adiabatic and long-wavelength limits of the magnetism theory. Both these approaches describe satisfactorily the magnetic interactions between Fe atoms, while the Rh atoms interactions are more sensitive to those approximations. We expect that our errors of J_{ij} determination and the corresponding errors in the estimation of the critical temperature of the magnetic phase transition are comparable with the quantum and magnetic short range order corrections.[25]

The obtained adiabatic long-wavelength parameters are shown in Table II. To estimate the magnetic contributions to the free energy we calculated the magnon spectrum in both phases. For the AFM state the spectrum is

$$\omega_{\mathbf{q}}^{\mathrm{AFM}} = (2g\mu_B/m_{\mathrm{Fe}})\sqrt{(J_0 - J_{\mathbf{q}})(J_0 - J_{\mathbf{q}+\mathbf{Q}})}, \qquad (1)$$

with $J_{\mathbf{q}} = \Sigma_j J_{ij} e^{i\mathbf{q}\cdot\mathbf{R}_{ij}}$ being the Fourier transformation of J_{ij} in AFM state and $\mathbf{Q} = (\pi\pi\pi)$. For the FM state

$$\omega_{\mathbf{q}}^{\mathrm{FM},\pm} = g\mu_B[A_{\mathbf{q}} + B_{\mathbf{q}} \pm \sqrt{(A_{\mathbf{q}} - B_{\mathbf{q}})^2 + 4X_{\mathbf{q}}^2}], \qquad (2)$$

where $A_{\mathbf{q}} = (J_0^{\mathrm{FeFe}} - J_{\mathbf{q}}^{\mathrm{FeFe}} + J_0^{\mathrm{FeRh}})/m_{\mathrm{Fe}}$, $B_{\mathbf{q}} = (J_0^{\mathrm{RhRh}} - J_{\mathbf{q}}^{\mathrm{RhRh}} + J_0^{\mathrm{FeRh}})/m_{\mathrm{Rh}}$, and $X_{\mathbf{q}} = J_{\mathbf{q}}^{\mathrm{FeRh}}/\sqrt{m_{\mathrm{Fe}} m_{\mathrm{Rh}}}$, with $J_{\mathbf{q}}^{\mathrm{FeFe}}$, $J_{\mathbf{q}}^{\mathrm{FeRh}}$, and $J_{\mathbf{q}}^{\mathrm{RhRh}}$ being the Fourier transformations of the exchange interactions inside (or between) the corresponding sublattice(s). The obtained magnon spectrum and DOS are shown in Fig. 2 together with the electronic DOS.

TABLE I. The calculated physical properties of the AFM and FM configurations of FeRh obtained in the local (first row) and nonlocal approximations. m_{Fe} and m_{Rh} are magnetic moments of Fe and Rh atoms, B is the bulk modulus, Θ_D is the Debye temperature, and $N(\epsilon_F)$ is DOS per formula unit at the Fermi level.

R_{WS} (a.u.)	ΔE (mRy/atom)	m_{Fe} (μ_B)	m_{Rh} (μ_B)	B (kbar)	Θ_D (K)	$N(\epsilon_F)$ (states/Ry)
2.767(2.780)	1.89	3.12(3.22)	0(1.04)	2454(2364)	385(379)	18.0(29.5)
2.796(2.807)	0.206	3.28(3.31)	0(1.02)	2194(2181)	366(365)	15.6(28.0)

TABLE II. The pair exchange parameters (in mRy) in AFM and FM phases of FeRh. Corresponding coordinates are shown in units of the lattice constant.

Type of pair	Δx	Δy	Δz	J_{ij}^{FM}	J_{ij}^{AF}
Fe—Rh	0.5	0.5	0.5	1.062	0
	1.5	0.5	0.5	0.058	0
	1	0	0	−0.098	0.442
Fe—Fe	1	1	0	0.104	0.008
	1	1	1	−0.479	0.603
	2	0	0	0.120	0.099
	2	1	0	0.045	0.005
Rh—Rh	1	0	0	0.086	0
	1	1	0	0.018	0

In order to study the relative stability of the AFM and FM configurations at finite temperatures, let us compare their free energies. We consider the contributions from electrons and magnons only. The lattice contribution is neglected because the magnitudes of the bulk moduli and Debye temperatures in both phases are very similar (Table I). The free energies due to band electrons and magnons are given by

$$F_{\mathrm{el}}(T) = \frac{1}{2}\left(\varepsilon_F n - k_B T \int d\varepsilon N(\varepsilon)\ln(1 + e^{(\varepsilon_F-\varepsilon)/k_BT})\right),$$

$$F_{\mathrm{mag}}(T) = -\frac{k_B T}{2}\int \frac{d\mathbf{q}}{(2\pi)^3}\ln(1 - e^{-\omega_{\mathbf{q}}/k_BT}), \qquad (3)$$

where n and $N(\varepsilon)$ are the number of electrons and the electronic DOS, correspondingly. Figure 3(a) shows the free energy difference $\Delta F = F^{\mathrm{FM}} - F^{\mathrm{AFM}}$ as a function of temperature. The transition temperature T_{tr}, determined from $\Delta F = 0$, is 371 K, which is close to the experimental result $T_{\mathrm{tr}} \approx 340$ K. Both contributions are shown, with the main one (more than 80%) coming from magnons. So, the origin of the AFM-FM transition should be attributed primarily to the magnon excitations rather than to pure electronic spectrum modifications. The obtained $\Delta F(T)$ also enables us to get the pressure dependence of the transition temperature, whose experimental value is about $dT_{\mathrm{tr}}/dP \approx 5.1-5.8$ K kbar^{-1}.[3,4] With applied pressure the AFM state gains more free energy $\Delta G = P\Delta V$ (ΔV is the volume difference) than the FM state and the derivative $d\Delta G/dP$ is close to -6.2×10^{-3} mRy kbar^{-1} per atom. From Fig. 3(a) $d\Delta F/dT = -1.17\times10^{-3}$ mRy K^{-1} at T_{tr} and from the equilibrium condition $d\Delta F = d\Delta G$, we obtain $dT_{\mathrm{tr}}/dP \approx 5.3$ K kbar^{-1}, which agrees well with the experiments.

From the obtained electronic DOS and magnon spectrum, one can also evaluate various thermal quantities. In Fig. 3(b) we show the calculated differences of the entropy and the specific heat between AFM and FM states as a function of temperature. These two quantities are independent of the zero temperature energy, with their measured values at T_{tr} being $\Delta S^{\mathrm{exp}} \approx 13-19.6$ J kg^{-1} K^{-1} (Refs. 7–9) and $\Delta C^{\mathrm{exp}} \approx 13.6$ J kg^{-1} K^{-1}.[8] Just as the free energy, the calculated contributions to both ΔS and ΔC near T_{tr} are mainly determined by the magnon excitations. At the calculated $T_{\mathrm{tr}} = 371$ K, we obtain $\Delta S = 19.3$ J kg^{-1} K^{-1} and $\Delta C = 15.1$ J kg^{-1} K^{-1}, while at $T_{\mathrm{tr}} \approx 340$ K, the corresponding values are 17.9 and 15.6 J kg^{-1} K^{-1}.

Since the Rh atoms have a nonzero value ($1\mu_B$) of magnetic moments in the FM state, this state has more magnetic degrees of freedom. It was proposed that these additional degrees increase the entropy and thus stabilize the FM state.[14] The evaluation of this entropy gain gives $\Delta S \approx Nk_B \ln 2 \approx 36$ J kg^{-1} K^{-1}, which is much larger than the experimental results. However, such picture of extra entropy is not quite accurate. From Figs. 2(b) and 2(c) one can see that in the FM state the magnon excitations $\omega_{\mathbf{q}}^{-}$ and $\omega_{\mathbf{q}}^{+}$ are

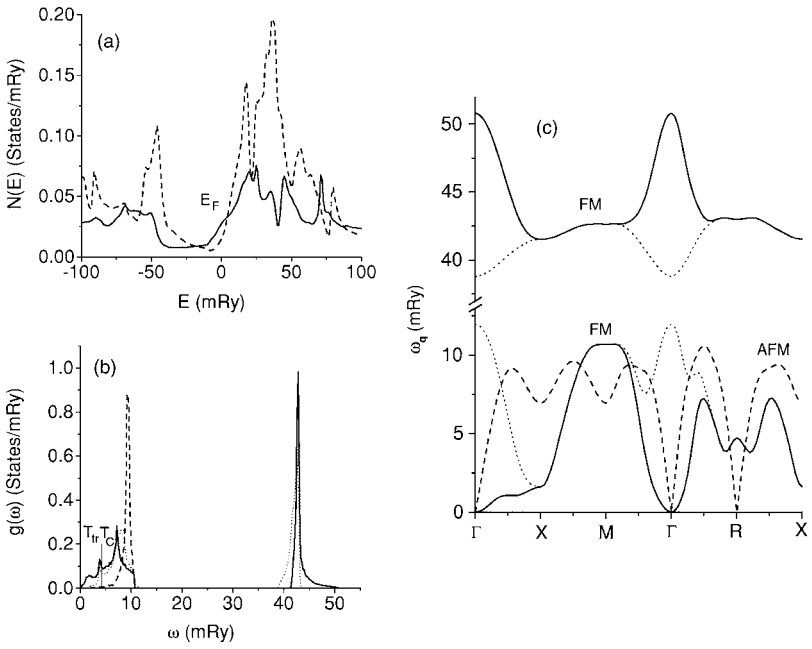

FIG. 2. The calculated DOS and magnon spectrum of FM (solid line) and AFM (dashed line) states: (a) the electronic DOS, (b) the magnon DOS, and (c) the magnon spectrum. In (b) and (c) the dotted lines correspond to the FM magnon DOS and spectrum when $X_{\mathbf{q}} = 0$ in the expression for $\omega_{\mathbf{q}}^{\mathrm{FM}}$.

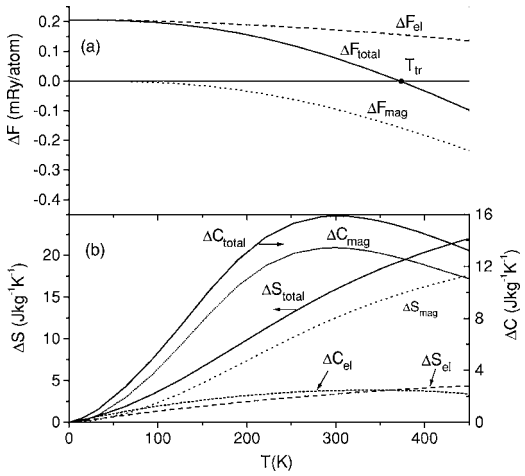

FIG. 3. The calculated differences of (a) the free energy ΔF and (b) the entropy ΔS and the specific heat ΔC between FM and AFM phases. The dashed and dotted lines (short-dashed and short-dotted lines for ΔC) correspond to the contributions from the electrons and magnons, respectively. The solid line is their sum.

separated by the large energy gap which reaches $2g\mu_B(m_{\mathrm{Fe}}^{-1}+m_{\mathrm{Rh}}^{-1})J_0^{\mathrm{FeRh}}\approx 51$ mRy at $\mathbf{q}=0$. We call the $\omega_{\mathbf{q}}^-$ ($\omega_{\mathbf{q}}^+$) mode to be Fe(Rh)-like, because a similar mode [the dotted lines in Figs. 2(b) and 2(c)] can be obtained if we fix the orientations of the Rh (Fe) moments by letting $X_{\mathbf{q}}=0$ in the expression for $\omega_{\mathbf{q}}^{\mathrm{FM}}$. Near $T_{\mathrm{tr}}(\approx 2.2$ mRy) only the Fe-like mode contributes to the thermal properties so that the number of effective magnon states in the FM and AFM phases is the same, i.e., there is essentially the same amount of spin degrees of freedom in the FM and AFM states. That does not mean, however, that the Rh moments in the FM phase do not contribute to the thermal properties. On Figs. 2(b) and 2(c) it is shown that without the Rh moments motion there is an energy gap between the ground state and the Fe-like magnons $\omega_{\mathbf{q}}^-$. Our calculation shows that at T_{tr} the free energy of magnons (with the orientations of the Rh moments being fixed) is only about one-third of that when they are not fixed. In other words, the movement of the Rh moments considerably affects the Fe-like magnon spectrum and thus significantly influences the thermal properties. Figure 2(c) also shows that around $\mathbf{q}=0$ the magnon stiffness in the FM state is much smaller than in the AFM state, so, near T_{tr} it is easier to excite magnons in the FM state. This can also be seen from Fig. 2(b), where the magnon DOS in the FM state is much larger than in the AFM state; the latter is in fact negligible for $\omega<3T_{\mathrm{tr}}$. As a result, when the temperature is increased, the free energy gain from magnon excitations in the FM state is increased much faster than in the AFM state. In our opinion, this is a main reason for the difference in thermal properties between those two phases and is also the driving force of the AFM-FM transition in FeRh.

Let us also evaluate the Curie temperature by using the obtained pair exchange interactions J_{ij}. In the mean field (MF) approximation

$$T_C^{\mathrm{MF}}=\frac{1}{3k_B}[J_0^{\mathrm{FeFe}}+J_0^{\mathrm{RhRh}}+\sqrt{(J_0^{\mathrm{FeFe}}-J_0^{\mathrm{RhRh}})^2+4(J_0^{\mathrm{FeRh}})^2}]. \tag{4}$$

From $J_0^{\mathrm{FeFe}}=-3.56$ mRy, $J_0^{\mathrm{FeRh}}=9.92$ mRy, and $J_0^{\mathrm{RhRh}}=0.85$ mRy we obtain 927 K, which is nearly 40% higher than the experimental $T_C\sim 670$ K. Our Monte Carlo calculations (with all calculated long-ranged J_{ij} included) produced correspondingly 660–690 K, so that the ratio $T_C/T_C^{\mathrm{MF}}\approx 0.71-0.74$ is nearly the same as for the simple cubic lattice where $T_C/T_C^{\mathrm{MF}}=0.722$.[26] The agreement of the calculated and the experimental T_C's indicates that the Heisenberg model may still work well in the temperature region near T_C in FeRh. However, all the results above have been obtained using classical spin statistics assuming small magnetic short range order. The inclusion of quantum corrections and magnetic short range order have mutually opposite influence on the critical temperature of the magnetic phase transition and require more detailed analysis. The corresponding studies we are planning to publish in our forthcoming papers.

RYG thanks Dr. G. D. Samolyuk for his help with the computational codes. This work was carried out at the Ames Laboratory, which is operated for the U.S. Department of Energy by Iowa State University under Contract No. W-7405-82. This work was supported by the Director for Energy Research, Office of Basic Energy Sciences of the U.S. Department of Energy.

[1] G. Shirane *et al.*, Phys. Rev. **134**, A1547 (1964).
[2] J. S. Kouvel and C. C. Hartelius, J. Appl. Phys. **33**, 1343 (1962).
[3] R. C. Wayne, Phys. Rev. **170**, 523 (1968).
[4] M. P. Annaorazov, J. Alloys Compd. **354**, 1 (2003).
[5] B. K. Ponomarev, Zh. Eksp. Teor. Fiz. **63**, 199 (1972) [Sov. Phys. JETP **36**, 105 (1973)].
[6] C. Kittel, Phys. Rev. **120**, 335 (1960).
[7] J. S. Kouvel, J. Appl. Phys. **37**, 1257 (1966).
[8] M. J. Richardson Phys. Lett. **46**, 153 (1973).
[9] M. P. Annaorazov *et al.*, J. Appl. Phys. **79**, 1689 (1996).
[10] P. Tu *et al.*, J. Appl. Phys. **40**, 1368 (1969).
[11] J. Ivarsson *et al.*, Phys. Lett. **35**, 167 (1971).
[12] L. Y. Chen and D. W. Lynch, Phys. Rev. B **37**, 10503 (1988).
[13] N. I. Kulikov *et al.*, J. Phys. F: Met. Phys. **12**, L91 (1982); C. Koenig, *ibid.* **12**, 1123 (1982).
[14] V. L. Moruzzi and P. M. Marcus, Phys. Rev. B **46**, 2864 (1992).
[15] A. Szajek and J. A. Morkowski, Physica B **193**, 81 (1994).
[16] M. E. Gruner *et al.*, Phys. Rev. B **67**, 064415 (2003).
[17] P. Bagno *et al.*, Phys. Rev. B **40**, R1997 (1989).
[18] T. Moriya, *Spin Fluctuations in Itinerant Electron Magnetism* (Springer, Berlin, 1985).
[19] H. L. Skriver, *The LMTO Method* (Spring-Verlag, Berlin, 1984).
[20] D. C. Langreth and M. J. Mehl, Phys. Rev. Lett. **47**, 446 (1981).
[21] V. Korenman *et al.*, Phys. Rev. B **16**, 4032 (1977); V. P. Antropov *et al.*, Phys. Rev. B **54**, 1019 (1996).
[22] V. P. Antropov *et al.*, Phys. Rev. Lett. **75**, 729 (1995).
[23] V. P. Antropov, J. Magn. Magn. Mater. **262**, L192 (2003).
[24] A. I. Liechtenstein *et al.*, J. Magn. Magn. Mater. **67**, 65 (1987).
[25] V. Antropov, cond-mat/0411393.
[26] P. Peczak *et al.*, Phys. Rev. B **43**, 6087 (1991).